



# Allosteric activation of proto-oncogene kinase Src by GPCR–beta-arrestin complexes

Received for publication, July 26, 2020, and in revised form, September 15, 2020. Published, Papers in Press, September 25, 2020, DOI 10.1074/jbc.RA120.015400

Natalia Pakharukova<sup>1</sup>, Ali Masoudi<sup>1</sup>, Biswaranjan Pani<sup>1</sup> , Dean P. Staus<sup>1</sup>, and Robert J. Lefkowitz<sup>1,2,3,\*</sup>

From the Departments of <sup>1</sup>Medicine and <sup>2</sup>Biochemistry, Duke University Medical Center, Durham, North Carolina, USA and the <sup>3</sup>Howard Hughes Medical Institute, Duke University Medical Center, Durham, North Carolina, USA

Edited by Henrik G. Dohlman

G protein–coupled receptors (GPCRs) initiate signaling cascades via G-proteins and beta-arrestins ( $\beta$ arr).  $\beta$ arr-dependent actions begin with recruitment of  $\beta$ arr to the phosphorylated receptor tail and are followed by engagement with the receptor core.  $\beta$ arrs are known to act as adaptor proteins binding receptors and various effectors, but it is unclear whether in addition to the scaffolding role  $\beta$ arrs can allosterically activate their downstream targets. Here we demonstrate the direct allosteric activation of proto-oncogene kinase Src by GPCR– $\beta$ arr complexes *in vitro* and establish the conformational basis of the activation. Whereas free  $\beta$ arr1 had no effect on Src activity,  $\beta$ arr1 in complex with M2 muscarinic or  $\beta$ 2-adrenergic receptors reconstituted in lipid nanodiscs activate Src by reducing the lag phase in Src autophosphorylation. Interestingly, receptor– $\beta$ arr1 complexes formed with a  $\beta$ arr1 mutant, in which the finger-loop, required to interact with the receptor core, has been deleted, fully retain the ability to activate Src. Similarly,  $\beta$ arr1 in complex with only a phosphorylated C-terminal tail of the vasopressin 2 receptor activates Src as efficiently as GPCR– $\beta$ arr complexes. In contrast,  $\beta$ arr1 and chimeric M2 receptor with nonphosphorylated C-terminal tail failed to activate Src. Taken together, these data demonstrate that the phosphorylated GPCR tail interaction with  $\beta$ arr1 is necessary and sufficient to empower it to allosterically activate Src. Our findings may have implications for understanding more broadly the mechanisms of allosteric activation of downstream targets by  $\beta$ arrs.

G protein–coupled receptors (GPCRs), the largest group of membrane proteins, regulate virtually all physiological processes and represent the most common drug targets (1). GPCRs translate various extracellular stimuli into specific cellular responses via activation of signal transducers: heterotrimeric G-proteins and beta-arrestins ( $\beta$ arr).  $\beta$ arrs, initially discovered as proteins that desensitize G-protein signaling (2, 3), are now recognized as signal transducers in their own right (reviewed in Ref. 4).

$\beta$ arr-dependent signaling begins with a two-step recruitment of  $\beta$ arr to the activated receptor. The first step involves binding to the phosphorylated receptor tail (5) (Fig. 1A) that converts  $\beta$ arr into an open active conformation characterized by, among other features, a 20-degree rotation between its N- and C-terminal domains (6). In addition, the C-edge loops of active  $\beta$ arr

interact with the lipid bilayer and function as a membrane anchor (7–9). The second step involves the engagement of the finger-loop region of  $\beta$ arr with the receptor core (10) (Fig. 1A). The bimodal binding of  $\beta$ arrs to GPCRs engenders the coexistence of two unique conformations of GPCR– $\beta$ arr complexes: the “tail” conformation and the “core” conformation, each with a distinct set of functions (11).

Upon activation by GPCRs,  $\beta$ arrs interact with a diverse set of partners including several mitogen-activated protein kinases and Src family tyrosine kinases (12, 13) among many others, and the physiological implications of these interactions are currently being explored in many laboratories. The nonreceptor tyrosine kinase Src is a pharmacologically important proto-oncogene, involved in the regulation of the cell cycle, adhesion, proliferation, and migration (reviewed in Ref. 14). It has been previously shown that  $\beta$ arr mediates the recruitment of Src to the activated  $\beta$ 2-adrenergic receptor and thus functions as an adaptor protein (12). In fact, Src was the very first signaling protein for which  $\beta$ arr was shown to serve such an adaptor role. Moreover, recent data suggest the possibility of direct allosteric effects of  $\beta$ arr on Src (15, 16). However, the molecular mechanisms and the conformational basis of these effects have not been elucidated. Herein, we use purified proteins to evaluate whether  $\beta$ arr can directly allosterically activate Src and to explore the conformational basis of such regulation.

## Results

### GPCR– $\beta$ arr1 complexes allosterically activate Src *in vitro* by promoting Src autophosphorylation

To study whether  $\beta$ arr1 directly activates Src *in vitro*, we expressed and purified Src,  $\beta$ arr1, and chimeric M2 muscarinic and  $\beta$ 2-adrenergic receptors (M2V2 and  $\beta$ 2V2, respectively). To ensure homogeneous phosphorylation, a synthetic phosphopeptide (V2Rpp) derived from the C-terminal tail of the vasopressin 2 (V2) receptor was ligated to the C termini of both receptors using sortase (17). V2Rpp has eight phosphorylated residues and confers tight binding to  $\beta$ arrs (6). M2V2 and  $\beta$ 2V2 were reconstituted in high-density lipoprotein particles (HDL, lipid nanodiscs) as this environment closely mimics a native membrane and enables testing functional outcomes in response to different ligands (Fig. 1B). We chose ~12-nm diameter MSP1D1E3 nanodiscs, previously found optimal for high-resolution structural studies of M2V2– $\beta$ arr1 complex (9). The extended lipid surface of MSP1D1E3 enables anchoring of C-domain of  $\beta$ arr1 to the lipid bilayer, which stabilizes the complex (9).

This article contains supporting information.

✂ Author's Choice—Final version open access under the terms of the Creative Commons CC-BY license.

\* For correspondence: Robert J. Lefkowitz, lefko001@receptor-biol.duke.edu.

This is an open access article under the CC BY license.

# Allosteric activation of Src by beta-arrestin 1

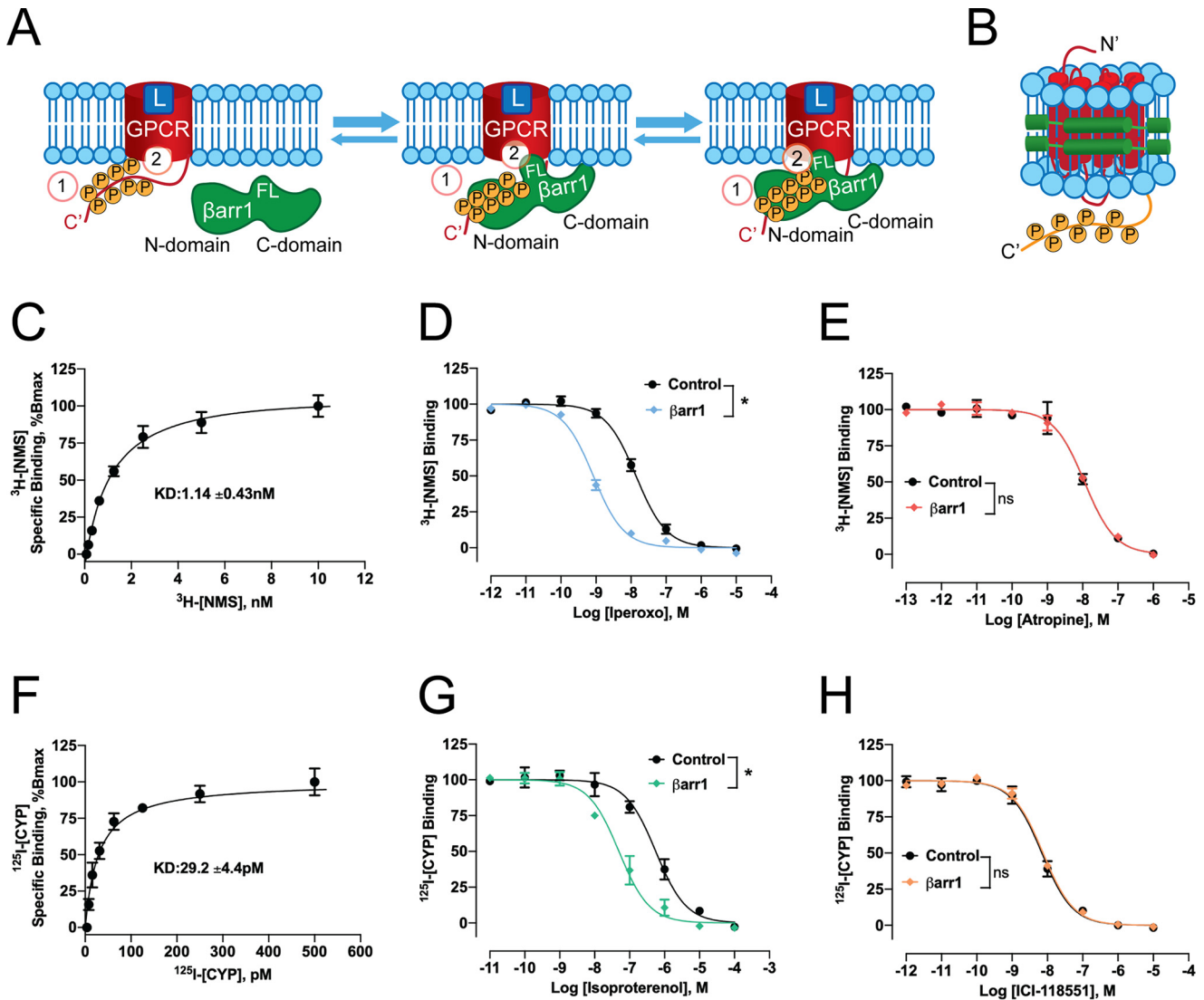
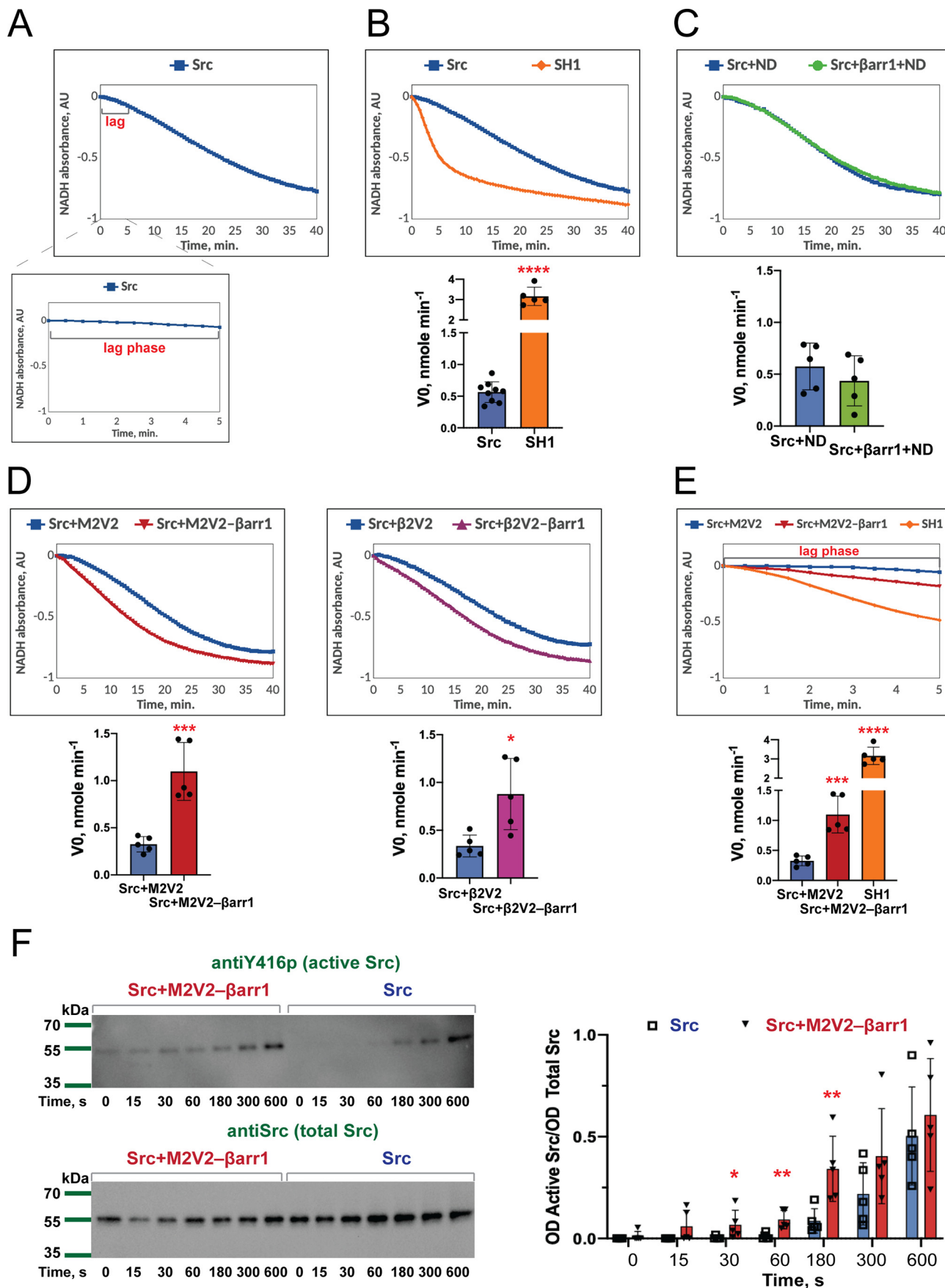


**Figure 1. Pharmacological characterization of M2V2 and  $\beta$ 2V2 reconstituted in lipid nanodiscs: ligand binding and allosteric coupling of  $\beta$ arr1.** *A*, schematic representation of GPCR– $\beta$ -arrestin1 binding:  $\beta$ arr1 recruitment begins with binding to the phosphorylated receptor tail (1) and is followed by the engagement with the receptor core (2). C-edge loops of active  $\beta$ arr1 anchor it to the membrane (L, ligand; FL, finger loop). *B*, schematic representation of chimeric M2 muscarinic (M2V2) and  $\beta$ 2-adrenergic (M2V2) receptors reconstituted in HDL particles (lipid nanodiscs). A synthetic phosphopeptide mimicking a phosphorylated C-terminal tail of V2 receptor was ligated to the receptors' C termini using sortase. The receptor is colored in red, the phosphorylated C-tail of V2 receptor is shown in yellow, MSP1D1E3 is shown in green. *C*, [ $^3$ H]NMS saturation ligand binding at HDL-M2V2. *D* and *E*, competition ligand binding assays using [ $^3$ H]NMS (1 nM) at HDL-M2V2 and a dose of agonist iperoxo (*D*) or antagonist atropine (*E*) in the absence (control) or presence of 1  $\mu$ M  $\beta$ arr1. *F*, [ $^{125}$ I]-CYP saturation ligand binding at HDL- $\beta$ 2V2. *G* and *H*, competition ligand binding assays using [ $^{125}$ I]-CYP (60 pM) at HDL- $\beta$ 2V2 and a dose of agonist isoproterenol (*G*) or antagonist ICI-118551 (*H*) in the absence (control) or presence of 1  $\mu$ M  $\beta$ arr1. *C*–*H*, points in respective curves represent mean  $\pm$  S.D. from three independent experiments. Asterisks (\*) in *B* and *E* indicate significant difference in IC<sub>50</sub> values between control versus  $\beta$ arr1 competition curves ( $p < 0.05$ , one-way ANOVA with Bonferroni's post test).

Ligand binding and allosteric coupling of  $\beta$ arr1 to HDL-reconstituted receptors were verified by radioligand-binding assays (Fig. 1, C–H). [ $^3$ H]NMS saturation ligand binding at HDL-M2V2 and [ $^{125}$ I]-CYP saturation ligand binding at HDL- $\beta$ 2V2 show apparent affinities of  $1.14 \pm 0.43$  nM and  $29.2 \pm 4.4$  pM for the respective radioligand (Fig. 1, C and F). Consistent with previous studies (17, 18), allosteric coupling of  $\beta$ arr1 results in a significant increase in agonist, but not antagonist, affinity at respective GPCRs (Fig. 1, D, E, G, and H).

We then measured the rate of phosphorylation of a synthetic peptide substrate (AEEIYGEFEAKKKK) by Src using a continuous kinase colorimetric assay (19). In this assay the rate of peptide phosphorylation is coupled via the pyruvate kinase/lac-

tate dehydrogenase enzymes to the oxidation of NADH measured through the decrease in absorbance at 340 nm. A progress curve of Src begins with a short lag phase with no or little changes in NADH absorbance (Fig. 2A). This lag phase is associated with the slow activation step caused by the disruption of an autoinhibited conformation of Src and intermolecular autophosphorylation of catalytic Tyr-416 (19). Once Src is fully activated, it quickly phosphorylates the substrate, which causes a rapid decrease in absorbance (Fig. 2A). The presence of lag phase in Src activity is clearly illustrated by comparing the progress curves of WT Src and a purified kinase domain of Src (SH1). SH1 represents a constitutively active form of the enzyme (20) and demonstrates no lag phase (Fig. 2B). Due to



## Allosteric activation of Src by beta-arrestin 1

the presence of the slow activation step, the Src kinetics before and during the activation process is divergent from Michaelis-Menten kinetics. Because the lag phase is indicative of the degree of autoinhibition of the enzyme, the initial velocity of the reaction ( $V_0$ ) represents the most accurate parameter to measure Src activity (21, 22).

We then performed the assay in the presence of  $\beta$ arr1 and GPCR- $\beta$ arr1 complexes. Whereas free  $\beta$ arr1 did not affect Src activity (Fig. 2C),  $\beta$ arr1 in complex with either phosphorylated M2V2 or  $\beta$ 2V2 activated by iperoxo or BI-167107, respectively, caused a significant increase in the rate of peptide phosphorylation by Src (Fig. 2D, Table S1). Addition of GPCR- $\beta$ arr1 complexes reduces this lag phase and leads to a more rapid decrease in absorbance (Fig. 2E). M2V2 and  $\beta$ 2V2 alone did not lead to Src activation (Fig. 2D) indicating that this process is mediated by  $\beta$ arr1. The initial velocity of peptide phosphorylation by SH1 is 5.6-fold higher than that of WT Src ( $3.16 \pm 0.45$  versus  $0.56 \pm 0.16$  nmol min<sup>-1</sup>, respectively), whereas in the presence of M2V2- $\beta$ arr1 and  $\beta$ 2V2- $\beta$ arr1 we observed a 3.4- and a 2.6-fold increase in the initial rate, respectively (Table S1). Taken together, our data demonstrate that receptor stimulated  $\beta$ arr1 directly activates Src.

Kinase assay data suggest that GPCR- $\beta$ arr1 complexes reduce the lag phase in Src activation (Fig. 2E). We thus hypothesized that interactions of GPCR- $\beta$ arr1 complexes with Src promotes Src autophosphorylation. To test this hypothesis, we analyzed the time course of Tyr-416 autophosphorylation by Western blotting (Fig. 2F). In the presence of the agonist-activated M2V2- $\beta$ arr1 complex, a phosphorylation of Tyr-416 was observed within 15–30 s after adding ATP, whereas for the Src alone reaction autophosphorylation was detected only at later time points. These data suggest that GPCR-stimulated  $\beta$ arr1 activates Src by reducing the lag phase in Src autophosphorylation.

## Phosphorylated GPCR tail interaction with $\beta$ -arrestin 1 is sufficient to confer the activation of Src

We next sought to elucidate which conformations of GPCR- $\beta$ arr complexes contribute to Src activation. Previously shown that  $\beta$ 2V2- $\beta$ arr1 complex represents a dynamic mixture of tail (partially engaged) and core (fully engaged) conformations (10). Recent structural and biophysical data demonstrate that in addition to tail and core interactions with the receptor, the C-edge of active  $\beta$ arr also engages the lipid nanodisc and functions as a membrane anchor (Figs. 1A and 3A) (8, 9).

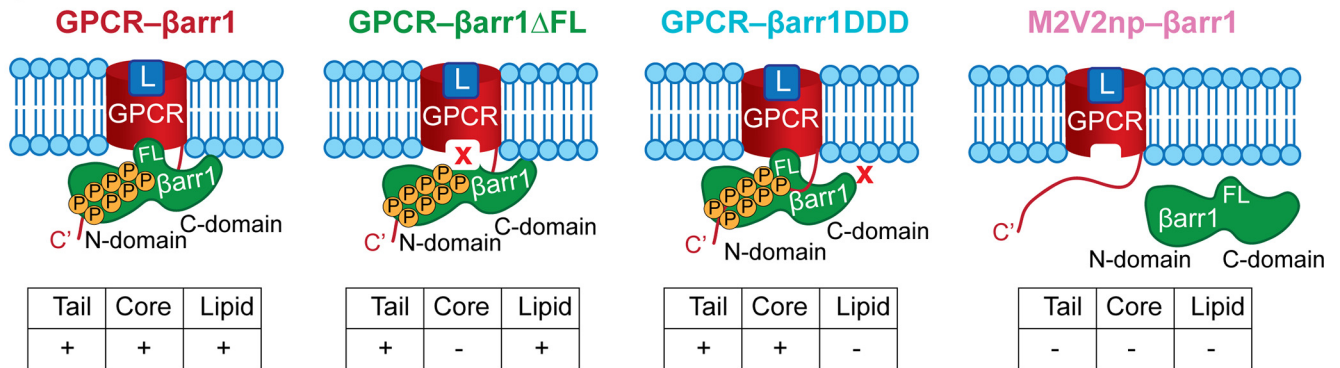
First, we tested whether an interaction of  $\beta$ arr1 with the receptor core is required for Src activation. Importantly, because C termini of both M2V2 and  $\beta$ 2V2 are phosphorylated,  $\beta$ arr1 will bind to the receptor tail regardless of the presence of an agonist. Interestingly, we observed full activation of Src even without agonist stimulation of  $\beta$ 2V2 (Fig. S1). This result suggests that allosteric activation of Src is primarily driven by interaction of  $\beta$ arr1 with the phosphorylated receptor tail. However, existing evidence of high (basal) constitutive activity of GPCR reconstituted in lipid nanodiscs (23) required additional experiments to verify this hypothesis.

To prevent  $\beta$ arr coupling to the receptor core, we expressed and purified a  $\beta$ arr1 mutant with a deleted finger loop ( $\beta$ arr1 $\Delta$ FL).  $\beta$ arr1 $\Delta$ FL is unable to interact with the receptor core (11), thus all GPCR- $\beta$ arr1 $\Delta$ FL complexes will remain in the tail conformation (Fig. 3A). Interestingly, both M2V2- $\beta$ arr1 $\Delta$ FL and  $\beta$ 2V2- $\beta$ arr1 $\Delta$ FL complexes fully retain the ability to activate Src suggesting that core interaction is dispensable for allosteric activation of the kinase (Figs. 3B).

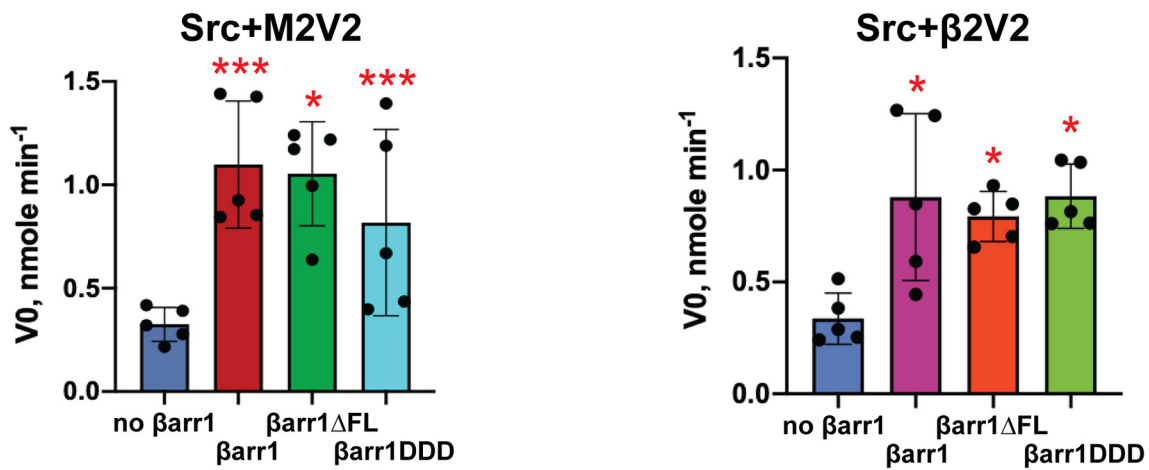
We next tested whether the engagement of  $\beta$ arr1 with the lipid bilayer plays a role in  $\beta$ arr1 ability to activate Src. Molecular dynamic simulations have shown that interactions between C-edge loops of  $\beta$ arr1 and the membrane stabilize the active

**Figure 2. GPCR-activated  $\beta$ arr 1 allosterically activates Src *in vitro* by reducing the lag phase in enzyme activation.** A, lag phase in Src activation: representative progress curve of NADH oxidation coupled to peptide phosphorylation by Src measured by continuous kinase colorimetric assay shown over the course 40 min (top panel) and during the first 5 min of reaction (bottom panel). Optimal Src peptide (AEEIYGEFEAKKKK) is used at a concentration of 250  $\mu$ M, Src was used at a concentration of 25 nM. B, constitutively active Src (SH1) shows no lag phase. Top panel: representative progress curves of NADH oxidation coupled to peptide phosphorylation by Src and SH1 measured by continuous kinase colorimetric assay. Bottom panel: initial velocity of peptide phosphorylation ( $V_0$ ) by Src and SH1. Individual data show mean  $\pm$  S.D. of five independent experiments (Src: 9 independent experiments). Statistical differences were determined by one-way ANOVA and Dunnett's multiple comparison test (\*\*\*\*,  $p < 0.0001$ ). Optimal Src peptide (AEEIYGEFEAKKKK) is used at a concentration of 250  $\mu$ M, Src and SH1 were used at a concentration of 25 nM. C,  $\beta$ arr1 alone does not have an effect on Src activity. Top panel: representative progress curves of NADH oxidation coupled to peptide phosphorylation by Src as measured by continuous kinase colorimetric assay. Bottom panel: initial velocity of peptide phosphorylation ( $V_0$ ). Individual data show mean  $\pm$  S.D. of five independent experiments. Statistical differences were determined by one-way ANOVA and Dunnett's multiple comparison test. Optimal Src peptide (AEEIYGEFEAKKKK) is used at a concentration of 250  $\mu$ M, Src was used at a concentration of 25 nM,  $\beta$ arr1 was used at a concentration of 125 nM. To reproduce the exact conditions of the experiment with GPCR- $\beta$ arr1 complexes, empty MSP1D1E3 (ND) nanodisc and Fab30 were added to Src at a concentration of 125 nM. D, M2V2- $\beta$ arr1 and  $\beta$ 2V2- $\beta$ arr1 complexes activate Src *in vitro*. Top panel: representative progress curves of NADH oxidation coupled to peptide phosphorylation by Src as measured by continuous kinase colorimetric assay. Bottom panel: initial velocity of peptide phosphorylation ( $V_0$ ). Individual data show mean  $\pm$  S.D. of five independent experiments. Statistical differences were determined by one-way ANOVA and Dunnett's multiple comparison test (\*,  $p < 0.05$ ; \*\*\*,  $p < 0.0005$ ). Optimal Src peptide (AEEIYGEFEAKKKK) was used at a concentration of 250  $\mu$ M and Src was used at a concentration of 25 nM. M2V2- $\beta$ arr1 and  $\beta$ 2V2- $\beta$ arr1 are used at a concentration of 125 nM. M2V2- $\beta$ arr1 and  $\beta$ 2V2- $\beta$ arr1 complexes are additionally stabilized by a synthetic antibody fragment Fab30 (125 nM). To reproduce the exact conditions of the experiment with GPCR- $\beta$ arr1 complexes, M2V2/ $\beta$ 2V2 and Fab30 were added to Src at a concentration of 125 nM. M2V2 was activated by iperoxo,  $\beta$ 2V2 was activated by BI-167107. E, GPCR-activated  $\beta$ arr1 reduces the lag phase in enzyme activity: Top panel: representative progress curves of NADH oxidation coupled to peptide phosphorylation by Src as measured by continuous kinase colorimetric assay during first 5 min of reaction. Bottom panel: initial velocity of peptide phosphorylation ( $V_0$ ). Optimal Src peptide (AEEIYGEFEAKKKK) is used at a concentration of 250  $\mu$ M, Src and SH1 were used at a concentration of 25 nM. M2V2- $\beta$ arr1 is used at a concentration of 125 nM. M2V2- $\beta$ arr1 complex is additionally stabilized by a synthetic antibody fragment Fab30 (125 nM). M2V2 was activated by iperoxo. To reproduce the exact conditions of the experiment with GPCR- $\beta$ arr1 complexes, M2V2/ $\beta$ 2V2 and Fab30 were added to Src at a concentration of 125 nM. M2V2 was activated by iperoxo,  $\beta$ 2V2 was activated by BI-167107. F, M2V2- $\beta$ arr1 complex promotes Src autophosphorylation. Left panel: time course of activation loop Tyr-416 autophosphorylation of Src *in vitro*. Representative Western blots are shown. Right panel: densitometry analysis of Tyr-416 phosphorylation expressed as a ratio over total Src (optical density of active Src/OD total Src). Src was used at a concentration of 12.5 nM and M2V2- $\beta$ arr1-Fab complexes were used at a concentration of 125 nM. Individual data show mean  $\pm$  S.D. of five independent experiments. Statistical differences were determined by Mann-Whitney test (\*,  $p < 0.05$ ; \*\*,  $p < 0.01$  as compared with the corresponding time point of Src alone reaction).

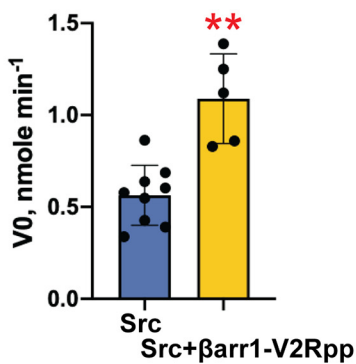
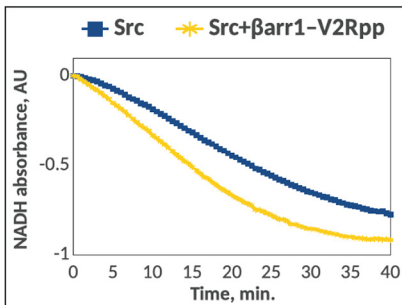
A



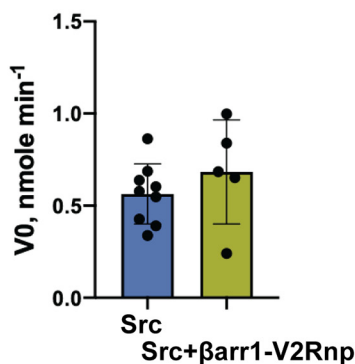
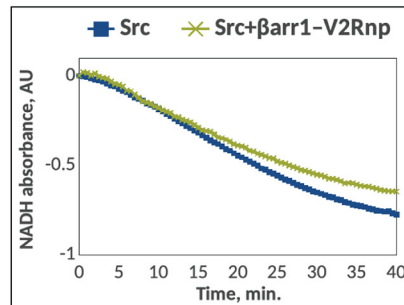
B



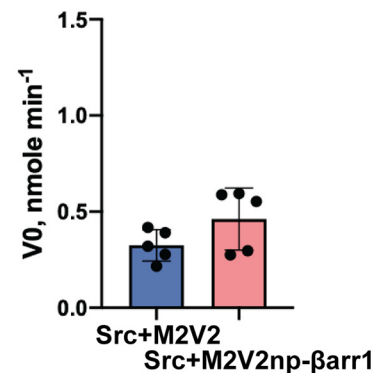
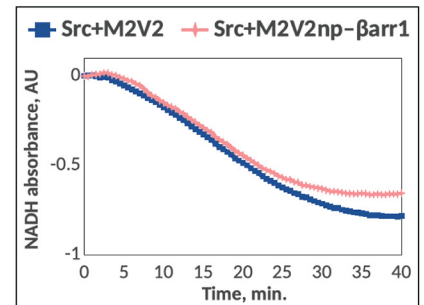
C



D



E



## Allosteric activation of Src by beta-arrestin 1

conformation of  $\beta$ arr1 (9) that might be crucial for allosteric activation of Src. We thus formed GPCR– $\beta$ arr complexes with a  $\beta$ arr1 mutant deficient in lipid interaction ( $\beta$ arr1DDD) (9) (Fig. 3A) and measured Src activity. M2V2– $\beta$ arr1DDD and  $\beta$ 2V2– $\beta$ arr1DDD complexes activate Src as efficiently as complexes formed with WT  $\beta$ arr1 and  $\beta$ arr1 $\Delta$ FL indicating that anchoring of  $\beta$ arr1 to the membrane is inessential for allosteric activation of the enzyme (Figs. 3B).

Our findings thus suggest that the interaction of  $\beta$ arr1 with a phosphorylated receptor tail is sufficient to allosterically activate Src. We then tested if active  $\beta$ arr1 with only a phosphorylated C-terminal tail of the V2 receptor ( $\beta$ arr1–V2Rpp) induces activation of Src similarly to GPCR– $\beta$ arr1 complexes. Indeed, we achieved the same level of Src activation in the presence of  $\beta$ arr1–V2Rpp and GPCR– $\beta$ arr1 (Fig. 3C, Table S1).

We next sought to ascertain whether phosphorylated GPCR tail interaction with  $\beta$ arr1 is absolutely required for allosteric activation of Src. We thus tested Src activity in the presence of  $\beta$ arr1 and nonphosphorylated C-terminal tail of the V2 receptor (V2Rnp) (Fig. 3D). As expected, no significant increase in Src activity was observed (Fig. 3D). Furthermore, the presence of  $\beta$ arr1 and nonphosphorylated M2V2 receptor (M2V2np) (Fig. 3A) also did not activate Src (Fig. 3E), probably due to the reduced binding of  $\beta$ arr1 to the nonphosphorylated receptor. To test the binding of  $\beta$ arr1 to both M2V2 and M2V2np, we performed a M1-FLAG pulldown assay (Fig. S2). Even though M2V2np binds a small amount of  $\beta$ arr1, it is not sufficient to trigger the activation of Src, as the large portion of  $\beta$ arr1 predominantly remains in an inactive conformation. Taken together, these data indicate that the phosphorylated GPCR tail interaction with  $\beta$ arr1 is necessary and sufficient to drive the allosteric activation of Src.

### $\beta$ -Arrestin 1 mediates allosteric activation of Src by interacting with SH3 domain

Our findings demonstrate that active  $\beta$ arr1 mediates allosteric activation of Src by promoting autophosphorylation of the enzyme. We next wanted to delineate the molecular mechanism of the activation. First, we tested the binding of active and inactive conformations of  $\beta$ arr1 to different regions of Src *in vitro* using a GSH S-transferase (GST)-pulldown assay (Fig. 4A).  $\beta$ arr1 weakly interacts with both SH3 and SH1 domains of Src, which is consistent with previously published data on  $\beta$ arr1–Src interactions in cells and *in vitro* (12, 13). Interest-

ingly, the SH3 domain of Src binds tighter to active  $\beta$ arr1 ( $\beta$ arr1–V2Rpp), whereas the SH1 domain interacts more strongly with the inactive form of  $\beta$ arr1 (Fig. 4A). To understand which of these interactions contribute to the allosteric activation of Src, we performed a competitive colorimetric kinase assay. In this assay we tested the ability of  $\beta$ arr1–V2Rpp to activate Src in the presence of an excess of either purified SH3 domain or a kinase dead mutant of the SH1 domain D386N (SH1 KD). The presence of SH1 KD does not impact the ability of  $\beta$ arr1–V2Rpp to activate Src (Fig. 4B). In contrast, an excess of SH3 domain completely blocks the  $\beta$ arr1-mediated activation of Src (Fig. 4B) suggesting that the SH3 domain binds to  $\beta$ arr1 and thus interferes with the mechanism of activation through direct competition with Src. Thus, the activation of Src by  $\beta$ -arrestins requires its interaction with the SH3 domain of the enzyme.

## Discussion

Arrestins play a plethora of roles in GPCR signaling. In addition to receptor desensitization, internalization, and intracellular trafficking, arrestins also function as independent signal transducers (reviewed in Ref. 4). However, the precise mechanisms of signal transduction via arrestins remain elusive. Here, we demonstrate that GPCR-activated  $\beta$ arr1 exerts direct allosteric activation of the proto-oncogene kinase Src *in vitro*.

$\beta$ arr-mediated effects on Src and extracellular signal regulated kinases (ERK1/2) have been explored in two recent studies (15, 16). In particular, it was shown that Src activation downstream of dopamine D1 receptor in HEK 293 cells solely depends on  $\beta$ arr2, whereas ERK1/2 activation involves both G-protein and  $\beta$ arr2 (16). Yang *et al.* (15) showed that  $\beta$ arr1 and GRK6-phosphorylated  $\beta$ 2-adrenergic receptor– $\beta$ arr1 complexes promoted Src activity *in vitro*. These studies, however, do not address the structural and conformational basis for the  $\beta$ arr-mediated allosteric activation of these enzymes. Here, we tested the contribution of five different conformational arrangements of  $\beta$ arr1 and GPCR– $\beta$ arr1 complexes to the activation of Src (Figs. 3A and 4C). With respect to receptor engagement these are: 1) fully engaged (tail-and-core of receptor are bound and  $\beta$ arr1 is membrane-anchored (M2V2– $\beta$ arr1); 2) fully receptor engaged  $\beta$ arr1-deficient in membrane interaction (M2V2– $\beta$ arr1DDD); 3) partially receptor engaged (tail-bound) membrane anchored (M2V2– $\beta$ arr1 $\Delta$ FL); 4) only receptor tail-bound ( $\beta$ arr1–V2Rpp); and 5) inactive  $\beta$ arr1:

**Figure 3. Phosphorylated GPCR tail interaction with  $\beta$ -arrestin 1 is sufficient to confer the activation of Src.** A, cartoon illustrating the effect of  $\beta$ arr1 mutations and receptor C-terminal tail phosphorylation on the conformation of GPCR– $\beta$ arr1 complexes. GPCR– $\beta$ arr1 complexes are additionally stabilized by a synthetic antibody fragment Fab30 (not shown for clarity) (L, ligand; FL, finger loop). B, interactions of  $\beta$ arr1 with the receptor core and with the lipid are dispensable for activation of Src. Initial velocity of peptide phosphorylation by Src as measured by continuous kinase colorimetric assay. Individual data show mean  $\pm$  S.D. of five independent experiments. Statistical differences were determined by one-way ANOVA and Dunnett's multiple comparison test (\*,  $p < 0.05$ ; \*\*\*,  $p < 0.0005$ ). Optimal Src peptide (AEEIYGEFEAKKKK) was used at a concentration of 250  $\mu$ M and Src used at a concentration of 25 nM. M2V2– $\beta$ arr1 and  $\beta$ 2V2– $\beta$ arr1 are used at a concentration of 125 nM. M2V2– $\beta$ arr1 and  $\beta$ 2V2– $\beta$ arr1 complexes are additionally stabilized by a synthetic antibody fragment Fab30 (125 nM). To reproduce the exact conditions of the experiment with GPCR– $\beta$ arr1 complexes, M2V2/ $\beta$ 2V2 and Fab30 were added to Src at a concentration of 125 nM. M2V2 was activated by iperoxo,  $\beta$ 2V2 was activated by BI-167107. C–E, receptor C-terminal tail phosphorylation is required for allosteric activation of Src. Representative progress curves of NADH oxidation coupled to peptide phosphorylation by Src, as measured by continuous kinase colorimetric assay (top panel) and initial velocity of peptide phosphorylation by Src (bottom panel), in the presence of  $\beta$ arr1–V2Rpp (C),  $\beta$ arr1–V2Rnp (D), or M2V2np– $\beta$ arr1 (E) are shown. Individual data show mean  $\pm$  S.D. of five independent experiments (Src: 9 independent experiments). Statistical differences were determined by one-way ANOVA and Dunnett's multiple comparison test (\*\*,  $p < 0.01$ ). Optimal Src peptide (AEEIYGEFEAKKKK) is used at a concentration of 250  $\mu$ M and Src was used at a concentration of 25 nM.  $\beta$ arr1–V2Rpp, M2V2np,  $\beta$ arr1, V2Rnp, and Fab30 are added at a concentration of 125 nM. To reproduce the exact conditions of the experiment with GPCR– $\beta$ arr1 complexes, M2V2 and Fab30 were added to Src at a concentration of 125 nM. M2V2np was activated by iperoxo.



## Allosteric activation of Src by beta-arrestin 1

$\beta$ arr1,  $\beta$ arr1-V2Rnp, and M2V2np- $\beta$ arr1. Apart from inactive  $\beta$ arr1, all conformations, including  $\beta$ arr1-V2Rpp, activate Src to a similar level, suggesting that the  $\beta$ arr1-mediated allosteric activation of Src depends only on the receptor tail-bound conformation of  $\beta$ arr1 and does not require its interaction with either the receptor core, or the membrane. Importantly, these findings suggest that initiation of signaling via  $\beta$ arrs may precede the termination of G-protein-mediated signaling, which requires  $\beta$ arr interaction with the receptor core. These results are also consistent with previously published data showing that the tail conformation of the  $\beta$ 2V2- $\beta$ arr1 complex retains the ability to mediate receptor internalization, a process known to be Src-dependent (11, 13, 24). Moreover, the interactions of  $\beta$ arr1 with the core of  $\beta$ 2V2 and V2 receptors are also dispensable for ERK2 binding and activation (24, 25). Interestingly, in contrast to the previously published work (15), we did not observe a statistically significant activation of Src in the presence of inactive  $\beta$ arr1. This result can be explained by a different  $\beta$ arr1:Src ratio (5:1 in our study *versus* 6:1 in Ref. 15) and slightly different conditions of the experiment. In addition, in the previous study (15) Src activity was determined by fitting the initial rate to the Michaelis-Menten equation to obtain  $K_m$  and  $k_{cat}$ , whereas we used the initial velocity to monitor the lag phase, similarly to previously published papers on activation of Src-family kinases (21, 22).

Intriguingly, we observed identical allosteric effects on Src by  $\beta$ arr1 stimulated by two different receptors, M2V2 and  $\beta$ 2V2, sharing the same phosphorylated V2 receptor tail and thus mimicking class B GPCRs. As shown previously (12, 15), WT  $\beta$ 2-adrenergic receptor, a class A GPCR, can also activate Src through  $\beta$ arr1 in an agonist and phosphorylation-dependent manner. These findings further buttress the conclusion that it is the phosphorylated receptor C terminus that orchestrates  $\beta$ arr1-mediated Src activation. Moreover, the phosphorylation pattern in the receptor tail is known to affect  $\beta$ arr-mediated recruitment of Src (15). In our study, nonphosphorylated M2V2np did not activate Src through  $\beta$ arr1 (Fig. 3E). These results support the barcode hypothesis, the notion that the receptor phosphorylation pattern induces a range of specific conformations of  $\beta$ arr1 that direct  $\beta$ arr1-mediated signaling (26, 27). It is therefore tempting to speculate that a receptor tail with a different phosphorylation pattern might elicit a different outcome on Src recruitment and activation even for the same receptor.

We found that GPCR-activated  $\beta$ arr1 reduces the lag phase in Src activation by promoting its trans-phosphorylation (Fig. 2, E and F). Furthermore, we showed that allosteric activation of Src requires the interaction of  $\beta$ arr1 with the SH3 domain of

the enzyme (Fig. 4B). The most plausible mechanism of the activation is therefore a disruption by  $\beta$ arr1-SH3 interactions of Src intramolecular contacts that normally constrain the activity of the kinase (Fig. 4C). SH3 domains recognize left-handed type II polyproline sequences PXXP (where X is any amino acid) (28). In an autoinhibited conformation of Src, the SH3 domain interacts with the type II helix of the linker between the SH2 and kinase domains (29) (Fig. 4C). This linker does not have the classical PXXP signature, therefore, a partner with an optimal polyproline sequence will easily displace the SH2 linker unlocking the autoinhibited conformation (30). This event represents a common mechanism of Src-family kinase activation and has been documented by several structural and biochemical studies (31, 32).

$\beta$ arr1 has three PXXP sequences ( $^{88}$ PPAP $^{91}$ ,  $^{121}$ PNLP $^{124}$ , and  $^{175}$ PERP $^{178}$ ), and previous studies have demonstrated that mutations of Pro-91 and Pro-121 drastically reduced  $\beta$ arr1-Src interactions and kinase activation (12, 15). It is currently unknown whether one particular site is involved in the interaction or they are inter-changeable. In a computationally generated docking model of GPCR- $\beta$ -arrestin-Src complex SH3 domain is positioned in the pocket between both Pro-91 and Pro-121 polyproline motifs of  $\beta$ arr1 (33). Intriguingly, none of the proline sites in  $\beta$ arr1 represent a canonical sequence for the SH3 domain of Src that requires consensus sequences RXXPPXXP or PXXPPXR, in which positively charged arginine is important for high affinity binding (28, 34, 35). Perhaps, due to the dynamic nature of the GPCR- $\beta$ arr1-Src signaling module low affinity interactions between SH3 and  $\beta$ arr1 are preferred. Further structural studies will shed light on the detailed molecular mechanism of Src recruitment and allosteric activation by  $\beta$ arrs.

In conclusion, we demonstrate that binding of  $\beta$ arr1 to the phosphorylated receptor tail instigates a distinct  $\beta$ arr1-mediated signaling pathway via allosteric activation of Src. A combination of biochemical approaches used in this study can easily be applied to explore allosteric activation of other downstream targets by  $\beta$ arr *in vitro*. Taken together, our findings represent an important step forward toward understanding more broadly the mechanisms of signal transduction via  $\beta$ arrs.

## Experimental procedures

### Molecular biology

Constructs expressing WT (residues 2-418) and a minimal cysteine (C59A, C125S, C140I, C150V, C242V, C251V, and C269S) and truncated ( $\beta$ arr1-MC-393) variants of rat  $\beta$ arr1 (17), Fab30 (36), human FLAG-M2 muscarinic and FLAG- $\beta$ 2-

**Figure 4. GPCR-activated  $\beta$ arr1 activates Src by interacting with its SH3 domain.** A,  $\beta$ arr1 interacts with SH3 and SH1 domains of Src. Left panel, GST-pull-down assay of SH3 domain and  $\beta$ arr1. Right panel, GST-pulldown assay of SH1 domain and  $\beta$ arr1. The right lane separated by a black line was spliced from a non-neighboring lane of the same blot. Data shown are representative of three independent experiments. B, addition of an excess of SH3 domain blocks  $\beta$ arr1-mediated activation of Src. Left and middle panels show representative progress curves of NADH oxidation coupled to peptide phosphorylation by Src in the presence of  $\beta$ arr1-V2Rpp and excess SH1 kinase dead (SH1 KD) (left panel) or SH3 domains (middle panel) measured by continuous kinase colorimetric assay. Right panel, initial velocity of peptide phosphorylation by Src in the presence of  $\beta$ arr1-V2Rpp and excess of SH3 or SH1 KD domains. Individual data show mean  $\pm$  S.D. of three independent experiments. Statistical differences were determined by Kruskal-Wallis test (one-way ANOVA on ranks) and Dunn's multiple comparison test (\*,  $p < 0.05$  as compared with Src alone). Optimal Src peptide (AEEIYGEFEAKKKK) is used at a concentration of 250  $\mu$ M, Src is used at a concentration of 200 nM, SH3 and SH1 KD are used at a concentration of 6  $\mu$ M.  $\beta$ arr1-V2Rpp (stabilized by Fab30) is used at a concentration of 1.2  $\mu$ M. C, conformational basis of  $\beta$ arr1-mediated activation of Src. Various tail-bound  $\beta$ arr1 conformations interact with SH3 domain of Src and disrupt the autoinhibited conformation of the enzyme (L, ligand; FL, finger loop).

adrenergic receptors with C-terminal sortase ligation consensus sequence (LPETGGH) and His<sub>6</sub> tag (17) have been reported previously. pHH0103\_SRC-1/1-IS2/2 plasmid used for the expression of the human Src SH3 domain (residues 87-144) was a gift from Sachdev Sidhu (Addgene plasmid 91251, RRID: Addgene\_91251) (37). Plasmids expressing WT chicken c-Src construct that contains the SH3, SH2, and SH1 kinase domains (residues 83-533, Src), kinase domain of WT chicken c-Src (residues 251-533, SH1), and YopH phosphatase were generous gifts from John Kuriyan. Mutations were introduced using QuikChange II site-directed mutagenesis kit (Agilent) and verified by Sanger sequencing.

### Protein expression and purification

The expression and purification of Src(83-533), SH1(251-533), and SH3(87-144) domains from *Escherichia coli* are described in details elsewhere (37, 38). Briefly, Src(83-533) and SH1(251-533) were co-expressed with YopH phosphatase and purified by immobilized metal ion affinity chromatography, anion exchange chromatography, and size-exclusion chromatography (SEC). SH3 was purified by immobilized metal ion affinity chromatography and SEC. WT  $\beta$ arr1 and its variants and Fab30 were expressed and purified as described previously (39, 40). The expression and purification of M2 receptor and  $\beta$ 2-adrenergic receptors containing an N-terminal FLAG tag, C-terminal sortase ligation consensus sequence (LPETGGH), and His<sub>6</sub> tag are described in details elsewhere (9, 17).

### Sortase ligation reactions and HDL reconstitution

Sortase ligation reaction and receptor reconstitution in high density lipoproteins (lipid nanodiscs) are described previously (9, 17). In brief, detergent-solubilized receptor (10  $\mu$ M) was incubated with a synthetic GGG-V2Rpp (GGG-ARGRpTPPPSLGPDpSCpTpTApSpSpSLAKDTSS) (50  $\mu$ M) or nonphosphorylated GGG-V2Rnp (50  $\mu$ M) and 2  $\mu$ M sortaseA in buffer containing 20 mM HEPES, pH 7.4, 100 mM NaCl, 0.1% *n*-dodecyl- $\beta$ -D-maltoside, 0.01% cholesteryl hemisuccinate, and 5 mM CaCl<sub>2</sub> overnight at 4 °C. Unligated receptor (containing C-terminal His-tag) and sortase were removed with Talon resin (Invitrogen). Prior to reconstitution, M2V2 and  $\beta$ 2V2 receptors (5  $\mu$ M) were incubated at 4 °C for 30 min with 2-fold molar excess of atropine or ICI-118551, respectively, and then for 1 h with 80  $\mu$ M membrane scaffold protein (MSP) MSP1D1E3 and a 3:2 molar ratio of 8 mM 1-palmitoyl-2-oleoyl-glycero-3-phosphocholine with 1-palmitoyl-2-oleoyl-*sn*-glycero-3-phospho-(1'-rac-glycerol). Subsequently Bio-Beads (Bio-Rad) were added (0.5 mg/ $\mu$ l of reconstitution volume) and incubation continued overnight at 4 °C with rotation. After reconstitution, HDL receptors were purified by M1-FLAG and SEC.

### Radioligand-binding assays

Saturation and competition radioligand-binding assays were performed at HDL-reconstituted M2V2 and  $\beta$ 2V2 (17, 18). All binding assays were carried out until equilibrium at room temperature in a buffer composed of 20 mM HEPES, pH 7.4, 100 mM NaCl, 0.2 mg/ml of BSA and 0.18 mg/ml of ascorbic acid.

For saturation ligand bindings a serial dilution of [<sup>3</sup>H]NMS (82 Ci/mmol; PerkinElmer) for M2V2 or <sup>125</sup>I-CYP (2,200 Ci/mmol; PerkinElmer) for  $\beta$ 2V2 was used. Nonspecific radioligand binding was assessed in parallel by including saturating concentrations of cold competitors, atropine (10  $\mu$ M) for M2V2 and propranolol (20  $\mu$ M) for  $\beta$ 2V2. For competition bindings, the displacement of [<sup>3</sup>H]NMS (1 nM) and <sup>125</sup>I-CYP (60 pM), at respective receptors, was determined by a serially diluted dose of cold agonist (iperoxo at 10<sup>-5</sup> to 10<sup>-12</sup> M; isoproterenol at 10<sup>-4</sup> to 10<sup>-11</sup> M) or antagonist (atropine at 10<sup>-6</sup> to 10<sup>-13</sup> M; ICI-118551 at 10<sup>-5</sup> to 10<sup>-12</sup> M), in the absence or presence of  $\beta$ arr1 at 1  $\mu$ M (6, 17). Binding reactions were harvested onto glass-fiber filters (GF/B), pre-soaked with 0.3% (v/v) polyethylenimine in deionized water using a 96-well Brandel harvester. Bound [<sup>3</sup>H] was extracted overnight with 5 ml of scintillation fluid and quantified using a Liquid Scintillation Analyzer Tri-Carb 2800TR (PerkinElmer), whereas bound <sup>125</sup>I was measured using a 2470 Wizard2<sup>TM</sup> 2-Detector Gamma Counter (PerkinElmer). Binding data were analyzed and plotted in GraphPad Prism using a nonlinear regression curve fit and a one-site specific binding equation to derive the estimates of the apparent maximum specific binding ( $B_{max}$ ), equilibrium binding constant ( $K_d$ ) and IC<sub>50</sub> for respective conditions. Statistical comparisons of respective IC<sub>50</sub> values were done by one-way analysis of variance (ANOVA) followed by a Bonferroni's multiple comparison post test and significance was determined at  $p < 0.05$ .

### Preparation of $\beta$ arr1-V2Rpp, M2V2- $\beta$ arr1, and $\beta$ 2V2- $\beta$ arr1 complexes

To prepare  $\beta$ arr1-V2Rpp complex,  $\beta$ arr1 was incubated with 2-fold molar excess of V2Rpp and Fab30 for 1 h at room temperature and then the complex was purified by SEC in 20 mM HEPES, pH 7.5, 150 mM NaCl, and 1 mM tris(2-carboxyethyl)phosphine hydrochloride (TCEP). To prepare M2V2- $\beta$ arr1 and  $\beta$ 2V2- $\beta$ arr1 complexes, M2V2 (20  $\mu$ M) and  $\beta$ 2V2 (20  $\mu$ M) receptors were preincubated with 5-fold molar excess of iperoxo or BI-167107, respectively, for 20 min on ice. After incubation, 20  $\mu$ M  $\beta$ arr1 and 20  $\mu$ M Fab30 were added and the mixture was incubated for 1 h on ice.

### Continuous colorimetric kinase assay

Continuous colorimetric kinase assay was performed as previously described (19). All reactions (200  $\mu$ l) contained Src, 100 mM HEPES, pH 7.5, 150 mM NaCl, 5 mM MgCl<sub>2</sub>, 1 mM phosphoenolpyruvate, 0.3 mM NADH, 0.25 mM optimal Src peptide (AEEIYGEFEAKKKK), 2 mM sodium orthovanadate, 1 mM TCEP, 0.005% Triton X-100, 4 units of pyruvate kinase, and 6 units of lactic dehydrogenase. The concentration of Src in all experiments was 25 nM and the concentration of  $\beta$ arr1 or GPCR- $\beta$ arr1 complex was 125 nM unless stated otherwise. In reactions containing  $\beta$ arr1,  $\beta$ arr1-V2Rpp, or GPCR- $\beta$ arr1 complexes, the reaction mixture was incubated for 1 h on ice. Reactions were started by the addition of ATP to a final concentration of 0.1 mM, and the decrease in NADH absorbance was monitored over 40 min at 25 °C using a CLARIOstar microplate reader (BMG Labtech). The initial velocity of the reaction

## Allosteric activation of Src by beta-arrestin 1

( $V_0$ ) was determined using a nonlinear regression curve fit in GraphPad Prism software. The change in absorbance was then converted to the product concentration using the Beer-Lambert law and to the amount of product formed in the reaction volume per minute. Statistical comparisons were determined by one-way ANOVA followed by a Dunnett's multiple comparison test.

### Src autophosphorylation assay

Src autophosphorylation reactions were performed as previously described (21). Src was diluted to 12.5 nM in a buffer containing 100 mM HEPES, pH 7.5, 150 mM NaCl, 5 mM MgCl<sub>2</sub>, 20 μg/ml of BSA, 2 mM sodium orthovanadate, and 1 mM TCEP. In reactions containing 125 nM M2V2-βarr1 complex, the reaction mixture was incubated for 1 h on ice before adding ATP. The reactions were initiated by addition of ATP to a final concentration of 0.1 mM and carried out on ice. At various time points, 50-μl aliquotes of the reaction were quenched with 15 μl of 4× SDS loading buffer and subjected to SDS-PAGE and Western blotting. The active form of Src was detected with anti-Src (phospho-Y418) antibody (Abcam, ab4816, 1:5000 dilution). The total Src was detected by anti-Src antibody (EMD Millipore 05-184, 1:2000 dilution) on a separate SDS-PAGE gel. The optical density of the bands was quantified in ImageJ and statistical differences were determined by Mann-Whitney test in GraphPad Prism software.

### M1-FLAG pulldown assay

To test the binding of βarr1 to M2V2 and M2V2np, 10 μM of the receptor was preincubated with a 5-fold molar excess of iperoxo and the positive allosteric modulator LY211,960 for 30 min on ice and then with a 2-fold molar excess of βarr1 and Fab30 for 2 h on ice. 50 μl of M1-FLAG resin equilibrated in 20 mM HEPES, pH 7.5, 100 mM NaCl buffer was added thereafter, and the mixture was rotated for 1 h at 4 °C and then additional 30 min after adding 2 mM CaCl<sub>2</sub>. After incubation the M1-FLAG beads were collected by centrifugation and washed with 20 mM HEPES, pH 7.5, 100 mM NaCl, 2 mM CaCl<sub>2</sub> buffer three times. The proteins were eluted with 0.2 mg/ml of FLAG-peptide and 5 mM EDTA in 20 mM HEPES, pH 7.5, 100 mM NaCl buffer. Receptor glycosylation was removed by incubation with a 1:10 protein ratio of peptide:N-glycosidase F to the receptor for 60 min at room temperature in the presence of 1% Nonidet P-40, 0.5% SDS, 40 mM DTT. The samples were subjected to SDS-PAGE, visualized by Instant Blue Coomassie stain (Expedon), and quantified by ImageJ.

### GST-pulldown assay

For detection of βarr1 binding to GST-SH3, 20 μM βarr1 was preincubated with 3-fold molar excess of V2Rpp and Fab30 for 1 h at room temperature, then 10 μM GST-SH3 was added and incubation continued for another 1 h. For detection of SH1 binding to GST-βarr1, 10 μM GST-βarr1 was preincubated with 3-fold molar excess of V2Rpp for 1 h at room temperature, then 20 μM SH1 was added and incubation continued for another 1 h. 50 μl of GST beads (GoldBio) equilibrated in 20 mM HEPES, pH 8.0, 150 mM NaCl buffer were added thereafter,

and the mixture incubated for 1 h at room temperature with rotation. After incubation the GST beads were collected by centrifugation and washed with 20 mM HEPES, pH 8.0, 150 mM NaCl buffer three times. The proteins were eluted from GST beads with 40 μl of 20 mM reduced GSH in 20 mM HEPES, pH 8.0, 150 mM NaCl buffer, then mixed with 4× SDS loading buffer, subjected to SDS-PAGE, and Western blotting and detected by EMD Millipore 05-184 antibody (SH3, 1:5000 dilution), Abcam ab1187 anti-His<sub>6</sub> tag antibody (SH1, 1:5000 dilution), and Cell Signaling Technology 30036S antibody (βarr1, 1:2000 dilution).

### Data availability

All data presented are available upon request from Robert J. Lefkowitz ([lefk001@receptor-biol.duke.edu](mailto:lefk001@receptor-biol.duke.edu)).

*Acknowledgments*—We thank Prof. John Kuriyan for helpful discussions throughout this work. We are grateful to Darrell Capel, Xingdong Zhang, and Xinrong Jiang for technical assistance and Yangyang Li, Quivetta Lennon, and Victoria Brennan for administrative assistance.

*Author contributions*—N. P. formal analysis; N. P., A. M., and B. P. investigation; N. P., A. M., B. P., and D. P. S. methodology; N. P. writing-original draft; A. M., B. P., D. P. S., and R. J. L. writing-review and editing; D. P. S. and R. J. L. conceptualization; R. J. L. data curation; R. J. L. supervision; R. J. L. funding acquisition.

*Funding and additional information*—This work was supported by National Institutes of Health Grant R01 HL16037 (to R. J. L.). R. J. L. is a Howard Hughes Medical Institute investigator. N. P. is supported by long-term postdoctoral fellowships from the Human Frontier Science Program and European Molecular Biology Organization. The content is solely the responsibility of the authors and does not necessarily represent the official views of the National Institutes of Health.

*Conflict of interest*—The authors declare that they have no conflicts of interest with the contents of this article.

*Abbreviations*—The abbreviations used are: GPCR, G-protein-coupled receptor; βarr, beta-arrestin; β2V2, β2-adrenergic receptor with phosphorylated C-terminal tail of V2 vasopressin receptor; ERK, extracellular signal-regulated kinase; GST, glutathione S-transferase; HDL, high-density lipoprotein; [<sup>3</sup>H]NMS, [<sup>3</sup>H]N-methylscopolamine; <sup>125</sup>I-CYP, <sup>125</sup>I-cyanopindolol; M2V2, M2 muscarinic receptor with phosphorylated tail of V2 vasopressin receptor; M2V2np, M2 muscarinic receptor with non-phosphorylated tail of V2 vasopressin receptor; MSP, membrane scaffold protein; OD, optical density; SEC, size-exclusion chromatography; SH1 KD, kinase-dead mutant of SH1 kinase domain of Src; TCEP, tris(2-carboxyethyl)phosphine hydrochloride; V2Rpp, V2 vasopressin receptor phosphopeptide; V2Rnp, V2 vasopressin receptor non-phosphorylated peptide; V2, vasopressin 2 receptor; SH, Src homology; ANOVA, analysis of variance.

## References

- Pierce, K. L., Premont, R. T., and Lefkowitz, R. J. (2002) Seven-transmembrane receptors. *Nat. Rev. Mol. Cell Biol.* **3**, 639–650 [CrossRef](#) [Medline](#)
- Benovic, J. L., Kühn, H., Weyand, I., Codina, J., Caron, M. G., and Lefkowitz, R. J. (1987) Functional desensitization of the isolated  $\beta$ -adrenergic receptor by the  $\beta$ -adrenergic receptor kinase: potential role of an analog of the retinal protein arrestin (48-kDa protein). *Proc. Natl. Acad. Sci. U.S.A.* **84**, 8879–8882 [CrossRef](#) [Medline](#)
- Lohse, M. J., Benovic, J. L., Codina, J., Caron, M. G., and Lefkowitz, R. J. (1990) Beta-arrestin: a protein that regulates beta-adrenergic receptor function. *Science* **248**, 1547–1550 [CrossRef](#) [Medline](#)
- Peterson, Y. K., and Luttrell, L. M. (2017) The diverse roles of arrestin scaffolds in G protein-coupled receptor signaling. *Pharmacol. Rev.* **69**, 256–297 [CrossRef](#) [Medline](#)
- Gimenez, L. E., Kook, S., Vishnivetskiy, S. A., Ahmed, M. R., Gurevich, E. V., and Gurevich, V. V. (2012) Role of receptor-attached phosphates in binding of visual and non-visual arrestins to G protein-coupled receptors. *J. Biol. Chem.* **287**, 9028–9040 [CrossRef](#) [Medline](#)
- Shukla, A. K., Manglik, A., Kruse, A. C., Xiao, K., Reis, R. I., Tseng, W. C., Staus, D. P., Hilger, D., Uysal, S., Huang, L. Y., Paduch, M., Tripathi-Shukla, P., Koide, A., Koide, S., Weis, W. I., *et al.* (2013) Structure of active  $\beta$ -arrestin-1 bound to a G-protein-coupled receptor phosphopeptide. *Nature* **497**, 137–141 [CrossRef](#) [Medline](#)
- Kang, Y., Zhou, X. E., Gao, X., He, Y., Liu, W., Ishchenko, A., Barty, A., White, T. A., Yefanov, O., Han, G. W., Xu, Q., de Waal, P. W., Ke, J., Tan, M. H., Zhang, C., *et al.* (2015) Crystal structure of rhodopsin bound to arrestin by femtosecond X-ray laser. *Nature* **523**, 561–567 [CrossRef](#) [Medline](#)
- Lally, C. C., Bauer, B., Selent, J., and Sommer, M. E. (2007) C-edge loops of arrestin function as a membrane anchor. *Nat. Commun.* **21**, 14258 [CrossRef](#)
- Staus, D. P., Hu, H., Robertson, M. J., Kleinhenz, A. L. W., Wingler, L. M., Capel, W. D., Latorraca, N. R., Lefkowitz, R. J., and Skiniotis, G. (2020) Structure of the M2 muscarinic receptor- $\beta$ -arrestin complex in a lipid nanodisc. *Nature* **579**, 297–302 [CrossRef](#) [Medline](#)
- Shukla, A. K., Westfield, G. H., Xiao, K., Reis, R. I., Huang, L. Y., Tripathi-Shukla, P., Qian, J., Li, S., Blanc, A., Oleskie, A. N., Dosey, A. M., Su, M., Liang, C. R., Gu, L. L., Shan, J. M., *et al.* (2014) Visualization of arrestin recruitment by a G-protein-coupled receptor. *Nature* **512**, 218–222 [CrossRef](#) [Medline](#)
- Cahill, T. J., III, Thomsen, A. R., Tarrasch, J. T., Plouffe, B., Nguyen, A. H., Yang, F., Huang, L. Y., Kahsai, A. W., Bassoni, D. L., Gavino, B. J., Lamerdin, J. E., Triest, S., Shukla, A. K., Berger, B., Little, J., 4th., *et al.* (2017) Distinct conformations of GPCR- $\beta$ -arrestin complexes mediate desensitization, signaling, and endocytosis. *Proc. Natl. Acad. Sci. U.S.A.* **114**, 2562–2567 [CrossRef](#) [Medline](#)
- Luttrell, L. M., Ferguson, S. S., Daaka, Y., Miller, W. E., Maudsley, S., Della Rocca, G. J., Lin, F., Kawakatsu, H., Owada, K., Luttrell, D. K., Caron, M. G., and Lefkowitz, R. J. (1999) Beta-arrestin-dependent formation of beta2 adrenergic receptor-Src protein kinase complexes. *Science* **283**, 655–661 [CrossRef](#) [Medline](#)
- Miller, W. E., Maudsley, S., Ahn, S., Khan, K. D., Luttrell, L. M., and Lefkowitz, R. J. (2000) Beta-Arrestin1 interacts with the catalytic domain of the tyrosine kinase c-SRC: role of beta-arrestin1-dependent targeting of c-SRC in receptor endocytosis. *J. Biol. Chem.* **275**, 11312–11319 [CrossRef](#) [Medline](#)
- Roskoski, R., Jr. (2015) Src protein-tyrosine kinase structure, mechanism, and small molecule inhibitors. *Pharmacol. Res.* **94**, 9–25 [CrossRef](#) [Medline](#)
- Yang, F., Xiao, P., Qu, C. X., Liu, Q., Wang, L. Y., Liu, Z. X., He, Q. T., Liu, C., Xu, J. Y., Li, R. R., Li, M. J., Li, Q., Guo, X. Z., Yang, Z. Y., He, D. F., *et al.* (2018) Allosteric mechanisms underlie GPCR signaling to SH3-domain proteins through arrestin. *Nat. Chem. Biol.* **14**, 876–886 [CrossRef](#) [Medline](#)
- Kaya, A. I., Perry, N. A., Gurevich, V. V., and Iverson, T. M. (2020) Phosphorylation barcode-dependent signal bias of the dopamine D1 receptor. *Proc. Natl. Acad. Sci. U.S.A.* **117**, 14139–14149 [CrossRef](#) [Medline](#)
- Staus, D. P., Wingler, L. M., Choi, M., Pani, B., Manglik, A., Kruse, A. C., and Lefkowitz, R. J. (2018) Sortase ligation enables homogeneous GPCR phosphorylation to reveal diversity in  $\beta$ -arrestin coupling. *Proc. Natl. Acad. Sci. U.S.A.* **115**, 3834–3839 [CrossRef](#) [Medline](#)
- Liu, X., Masoudi, A., Kahsai, A. W., Huang, L. Y., Pani, B., Staus, D. P., Shim, P. J., Hirata, K., Simhal, R. K., Schwab, A. M., Rambarat, P. K., Ahn, S., Lefkowitz, R. J., and Kobilka, B. (2019) Mechanism of  $\beta$ 2AR regulation by an intracellular positive allosteric modulator. *Science* **364**, 1283–1287 [CrossRef](#) [Medline](#)
- Barker, S. C., Kassel, D. B., Weigl, D., Huang, X., Luther, M. A., and Knight, W. B. (1995) Characterization of pp60c-src tyrosine kinase activities using a continuous assay: autoactivation of the enzyme is an intermolecular autophosphorylation process. *Biochemistry* **34**, 14843–14851 [CrossRef](#) [Medline](#)
- Seidel-Dugan, C., Meyer, B. E., Thomas, S. M., and Brugge, J. S. (1992) Effects of SH2 and SH3 deletions on the functional activities of wild-type and transforming variants of c-Src. *Mol. Cell Biol.* **12**, 1835–1845 [CrossRef](#) [Medline](#)
- Shah, N. H., Wang, Q., Yan, Q., Karandur, D., Kadlecsek, T. A., Fallahee, I. R., Russ, W. P., Ranganathan, R., Weiss, A., and Kuriyan, J. (2016) An electrostatic selection mechanism controls sequential kinase signaling downstream of the T cell receptor. *Elife* **5**, e20105 [CrossRef](#)
- Shah, N. H., Löbel, M., Weiss, A., and Kuriyan, J. (2018) Fine-tuning of substrate preferences of the Src-family kinase Lck revealed through a high-throughput specificity screen. *Elife* **7**, e35190 [CrossRef](#)
- Staus, D. P., Wingler, L. M., Pichugin, D., Prosser, R. S., and Lefkowitz, R. J. (2019) Detergent- and phospholipid-based reconstitution systems have differential effects on constitutive activity of G-protein-coupled receptors. *J. Biol. Chem.* **294**, 13218–13223 [CrossRef](#) [Medline](#)
- Kumari, P., Srivastava, A., Banerjee, R., Ghosh, E., Gupta, P., Ranjan, R., Chen, X., Gupta, B., Gupta, C., Jaiman, D., and Shukla, A. K. (2016) Functional competence of a partially engaged GPCR- $\beta$ -arrestin complex. *Nat. Commun.* **7**, 13416 [CrossRef](#) [Medline](#)
- Kumari, P., Srivastava, A., Ghosh, E., Ranjan, R., Dogra, S., Yadav, P. N., and Shukla, A. K. (2017) Core engagement with  $\beta$ -arrestin is dispensable for agonist-induced vasopressin receptor endocytosis and ERK activation. *Mol. Biol. Cell* **28**, 1003–1010 [CrossRef](#) [Medline](#)
- Kim, J., Ahn, S., Ren, X. R., Whalen, E. J., Reiter, E., Wei, H., and Lefkowitz, R. J. (2005) Functional antagonism of different G protein-coupled receptor kinases for beta-arrestin-mediated angiotensin II receptor signaling. *Proc. Natl. Acad. Sci. U.S.A.* **102**, 1442–1447 [CrossRef](#) [Medline](#)
- Nobles, K. N., Xiao, K., Ahn, S., Shukla, A. K., Lam, C. M., Rajagopal, S., Strachan, R. T., Huang, T. Y., Bressler, E. A., Hara, M. R., Shenoy, S. K., Gygi, S. P., and Lefkowitz, R. J. (2011) Distinct phosphorylation sites on the  $\beta(2)$ -adrenergic receptor establish a barcode that encodes differential functions of  $\beta$ -arrestin. *Sci. Signal.* **4**, ra51 [CrossRef](#) [Medline](#)
- Mayer, B. J., and Eck, M. J. (1995) SH3 domains: minding your p's and q's. *Curr. Biol.* **5**, 364–367 [CrossRef](#) [Medline](#)
- Xu, W., Doshi, A., Lei, M., Eck, M. J., and Harrison, S. C. (1999) Crystal structures of c-Src reveal features of its autoinhibitory mechanism. *Mol. Cell.* **3**, 629–638 [CrossRef](#) [Medline](#)
- Harrison, S. C. (2003) Variation on an Src-like theme. *Cell* **112**, 737–740 [CrossRef](#)
- Lee, C. H., Saksela, K., Mirza, U. A., Chait, B. T., and Kuriyan, J. (1996) Crystal structure of the conserved core of HIV-1 Nef complexed with a Src family SH3 domain. *Cell* **85**, 931–942 [CrossRef](#) [Medline](#)
- Moarefi, I., LaFevre-Bernt, M., Sicheri, F., Huse, M., Lee, C. H., Kuriyan, J., and Miller, W. T. (1997) Activation of the Src-family tyrosine kinase Hck by SH3 domain displacement. *Nature* **385**, 650–653 [CrossRef](#) [Medline](#)
- Bourquard, T., Landomiel, F., Reiter, E., Crépieux, P., Ritchie, D. W., Azé, J., and Poupon, A. (2015) Unraveling the molecular architecture of a G protein-coupled receptor/ $\beta$ -arrestin/Erk module complex. *Sci. Rep.* **5**, 10760 [CrossRef](#) [Medline](#)
- Feng, S., Chen, J. K., Yu, H., Simon, J. A., and Schreiber, S. L. (1994) Two binding orientations for peptides to the Src SH3 domain: development of a general model for SH3–ligand interactions. *Science* **266**, 1241–1247 [CrossRef](#) [Medline](#)

## Allosteric activation of Src by beta-arrestin 1

35. Alexandropoulos, K., Cheng, G., and Baltimore, D. (1995) Proline-rich sequences that bind to Src homology 3 domains with individual specificities. *Proc. Natl. Acad. Sci. U.S.A.* **92**, 3110–3114 [CrossRef Medline](#)
36. Paduch, M., Koide, A., Uysal, S., Rizk, S. S., Koide, S., and Kossiakoff, A. A. (2013) Generating conformation-specific synthetic antibodies to trap proteins in selected functional states. *Methods* **60**, 3–14 [CrossRef Medline](#)
37. Teyra, J., Huang, H., Jain, S., Guan, X., Dong, A., Liu, Y., Tempel, W., Min, J., Tong, Y., Kim, P. M., Bader, G. D., and Sidhu, S. S. (2017) Comprehensive analysis of the human SH3 domain family reveals a wide variety of non-canonical specificities. *Structure* **25**, 1598–1610 [CrossRef Medline](#)
38. Seeliger, M. A., Young, M., Henderson, M. N., Henderson, N., Pellicena, P., King, D. S., Falick, A. M., and Kuriyan, J. (2005) High yield bacterial expression of active c-Abl and c-Src tyrosine kinases. *Protein Sci.* **14**, 3135–3139 [CrossRef Medline](#)
39. Nobles, K. N., Guan, Z., Xiao, K., Oas, T. G., and Lefkowitz, R. J. (2007) The active conformation of beta-arrestin1: direct evidence for the phosphate sensor in the N-domain and conformational differences in the active states of beta-arrestins1 and -2. *J. Biol. Chem.* **282**, 21370–21381 [CrossRef Medline](#)
40. Rizk, S. S., Paduch, M., Heithaus, J. H., Duguid, E. M., Sandstrom, A., and Kossiakoff, A. A. (2011) Allosteric control of ligand-binding affinity using engineered conformation-specific effector proteins. *Nat. Struct. Mol. Biol.* **18**, 437–442 [CrossRef Medline](#)